CHAPTER 5. DEVELOPMENT OF PREDICTION MODELS

This chapter develops three prediction models to forecast the chaotic traffic flow time-series data: (1) the temporal confined (TC) model, which uses temporal similarity for the prediction reasoning; (2) the spatiotemporal confined (STC) model, which incorporates both spatial and temporal similarities into the prediction reasoning; (3) the spatial confined (SC) model, which employs spatial similarity for the prediction reasoning. This chapter is organized as follows: In Section 5.1, details the proposed three models. Section 5.2 carries out an empirical study. The prediction performances by these three models are compared. Section 5.3 further conducts sensitivity analyses by varying the spatial or temporal threshold values.

5.1 Proposed Models

5.1.1 Temporal Confined (TC) Model

Our first prediction model is established on the basis of "temporal confined (TC)" reasoning concept; thus is termed as TC model. To explain the TC reasoning, we plot several trajectories as shown in Figure 5-1, of which the patterns of two historical vectors $\mathrm{Z}_2(t)$ and $\mathrm{Z}_4(t)$ are assumed "significantly dissimilar" from the current observed vector $\mathrm{Z}_p(t)$; namely, $\left|\xi_{2n}(t)-\xi_{2n}(t-v)\right|$ and $\left|\xi_{4n}(t)-\xi_{4n}(t-v)\right|$ are significantly larger than $\left|\xi_{pn}(t)-\xi_{pn}(t-v)\right|$ in the n^{th} dimensional state space, then our TC reasoning will exclude these two vectors from being selected for the future change reasoning from $\mathrm{Z}_p(t)$ to $\mathrm{Z}_p(t+s)$.

The "temporal similarity" refers to the situation when the gap of differencing variable between $\zeta_{pn}(t)$ and $\zeta_{mn}(t)$ is smaller than a designated temporal threshold value (ε_t). In other words, all the historical trajectories are viewed as similar if their temporal changes are within the temporal sphere confined by a temporal threshold ε_t. For the historical trajectories with temporal changes greater than ε_t, they will not be chosen for the prediction reasoning. Theoretically, the smaller the threshold value ε_t

is, the easier it is to find the trajectories that are similar to the changes of the present vector trajectories to serve as the basis of future change reasoning. However, if ε_t is too small, the data might be insufficient to find similar trajectories because too many historical observations might be excluded. If ε_t is too big, the prediction accuracy might be compromised. In the present paper, we do not attempt to determine the optimal temporal threshold value.

We will assign various weights to the differencing variables of historical observations based on the "degrees of similarity" and then multiply them respectively by the differencing variables of the future state to estimate the weighted average of increment for the future change reasoning. Once the increment is estimated, the value in the future state of the present time series can be predicted. Detailed procedures for the proposed TC model are explained as follows:

Step 1. Data preprocessing

Plot the time series data $Z_p(t)$ of the latest observations in the N-dimensional reconstructed state space.

$$Z_p(t) = \{\zeta_{pn}[t-(n-1)\tau],\ \mathrm{n}=1,2,\ldots,\mathrm{N}\} \tag{5-1}$$

Step 2. Feature extraction

Calculate the "past" temporal differencing values of the latest observations $Z_p(t)$ and of the m historical observations $Z_m(t)$ at v steps ahead by eqs. (5-2) and (5-3), respectively.

$$\Delta\theta_{pn}(t) = \zeta_{pn}(t) - \zeta_{pn}(t-v),\ n = 1,2,\ldots,N \tag{5-2}$$

$$\Delta\theta_{mn}(t) = \zeta_{mn}(t) - \zeta_{mn}(t-v),\ n = 1,2,\ldots,N;\ m = 1,2,\ldots,M \tag{5-3}$$

Step 3. Define the similarity by a temporal threshold

Figure 5-1 illustrates a temporal sphere confined by a temporal threshold ε_t. We investigate all the historical observations that have "temporal similarity" to the latest observations. Any historical observations that are within the confined sphere are selected as references for prediction reasoning. Namely, choose the historical observations with differencing values of $\Delta\theta_{pn}(t)$ and $\Delta\theta_{mn}(t)$ smaller than ε_t as calculated in eq. (5-4).

$$\left|\Delta\theta_{pn}(t)-\Delta\theta_{mn}(t)\right| \le \varepsilon_t \text{, m=1, 2,…, M; n=1, 2,…, N} \tag{5-4}$$

In Figure 5-1, for example, $Z_1(t)$, $Z_3(t)$ and $Z_M(t)$ are selected because their differencing values of $\Delta\theta_{pn}(t)$ and $\Delta\theta_{mn}(t)$ are smaller than ε_t; however, $Z_2(t)$ and $Z_4(t)$ are not selected because their differencing values are larger than ε_t. Let M_1' denote the number of the historical observations being selected by the screening through temporal threshold ε_t.

Step 4. Perform the reasoning

IF $\left|\Delta\theta_{pn}(t)-\Delta\theta_{mn}(t)\right| \le \varepsilon_t$, THEN $\Delta\theta_{pn}(s)$ is "fuzzy equal" to $\Delta\theta_{mn}(s)$ (5-5)

Step 5. Calculate the similarity membership degrees

Figure 5-2 illustrates the triangle membership functions, which are consisted of three differencing values, $\Delta\theta_{1n}(t)$, $\Delta\theta_{3n}(t)$, $\Delta\theta_{Mn}(t)$. Each membership degree (ω_{mn}) can be estimated by its membership function as follows:

$$\omega_{mn}=\frac{\varepsilon_t}{\Delta\theta_{pn}(t)+\varepsilon_t-\Delta\theta_{mn}(t)} \tag{5-6}$$

Step 6. Estimate the "increments" for prediction

Calculate the future differencing values for the latest observations. Use eq. (5-7) to calculate the estimator $\Delta\hat{\theta}_{TC}(s)$ from the differencing value $\Delta\theta_{mn}(s)$ obtained from eq. (5-5).

$$\Delta\hat{\theta}_{TC}(s) = \frac{\sum_{m=1}^{M_1'} \omega_{mn} \Delta\theta_{mn}(s)}{\sum_{m=1}^{M_1'} \omega_{mn}} \tag{5-7}$$

Step 7. Compute the predicted values for the latest observations

$$\hat{\zeta}_{pn}(t+s) = \zeta_{pn}(t) + \Delta\hat{\theta}_{TC}(s) \tag{5-8}$$

5.1.2 Spatiotemporal Confined (STC) Model

Our second prediction model is established on the basis of “spatial and temporal confined (STC)” reasoning concept and hence termed as STC model. The STC model is in effect to further impose a spatial limitation on the TC model. In other words, the TC model only set up a temporal sphere in selecting the similar trajectories; however, the STC model set up both temporal and spatial spheres to screen the historical trajectories for prediction reasoning. Detailed procedures for the proposed STC model are explained as follows:

Step 1. Data preprocessing

Plot the time series data $Z_p(t)$ of the latest observations in the *N*-dimensional reconstructed state space as the TC model does.

Step 2. Feature extraction

Calculate the “past” temporal differencing values of the latest observations $Z_p(t)$ and of the *m* historical observations $Z_m(t)$ at *v* steps ahead as the TC model does.

Step 3. Define the similarity by spatial and temporal thresholds

Two threshold values, spatial threshold (ε_s) and temporal threshold (ε_t), are used to define the "similar trajectories" as shown in Figure 5-3. For the spatial confined reasoning, select historical observations whose $Z_p(t) - Z_m(t)$ are smaller than ε_s. Namely,

$$\left|\zeta_{pn}[t-(n-1)\tau] - \zeta_{mn}[t-(n-1)\tau]\right| \le \varepsilon_1,\ m\text{=1, 2,…, M; } n\text{=1, 2,…, N} \qquad (5\text{-}9)$$

For example, $Z_1(t)$, $Z_2(t)$, $Z_3(t)$ and $Z_4(t)$ in Figure 5-2 are selected because they are within the spatial threshold. $Z_M(t)$ is excluded because $Z_p(t) - Z_M(t)$ is larger than the spatial threshold value ε_s. For the temporal confined reasoning, a temporal threshold (ε_t) is further applied. As explained in the TC model case, $Z_2(t)$ and $Z_4(t)$ are excluded because their differencing values of $\Delta\zeta_{pn}(t)$ and $\Delta\zeta_{mn}(t)$ are larger than the temporal threshold value ε_t. Let M_2' be the number of the historical observations being selected by the screening through thresholds ε_s and ε_t.

Step 4. Perform the reasoning

IF $\left|\zeta_{pn}[t-(n-1)\tau] - \zeta_{mn}[t-(n-1)\tau]\right| \le \varepsilon_s$ AND $\left|\Delta\zeta_{pn}(t) - \Delta\zeta_{mn}(t)\right| \le \varepsilon_t$

THEN $\Delta\zeta_{pn}(s)$ is "fuzzy equal" to $\Delta\zeta_{mn}(s)$ (5-10)

Step 5. Calculate the similarity membership degrees

Figure 5-4 demonstrates the triangle similarity membership functions which are consisted of two differencing values, $\Delta\theta_{1n}(t)$ and $\Delta\theta_{3n}(t)$. Each membership degree (ω_{mn}) can be estimated by its membership function, also from eq. (5-6).

Step 6. Estimate the "increments" for prediction

Calculate the future differencing values for the latest observations. Use eq. (5-11) to calculate the estimator $\Delta\hat{\theta}_{STC}(s)$ from the differencing value $\Delta\theta_{mn}(s)$ obtained from eq. (5-10).

$$\Delta\hat{\theta}_{STC}(s) = \frac{\sum_{m=1}^{M_2'} \omega_{mn} \Delta\theta_{mn}(s)}{\sum_{m=1}^{M_2'} \omega_{mn}} \tag{5-11}$$

Step 7. Compute the predicted values for the latest observations

$$\hat{\zeta}_{pn}(t+s) = \zeta_{pn}(t) + \Delta\hat{\theta}_{STC}(s) \tag{5-12}$$

5.1.3 Spatial Confined (SC) Model

The third prediction model is established on the basis of “spatial confined (SC)” reasoning concept and therefore termed as SC model. We only set up a spatial constraint to screen the historical similar trajectories for the prediction reasoning; however, the reasoning for the SC model is different from the above two models. Detailed procedures for the proposed SC model are explained as follows:

Step 1 Data preprocessing

Plot the time series data $Z_p(t)$ of the latest observations in the N-dimensional reconstructed state space as the TC model does.

Step 2. Feature extraction

Calculate the “past” temporal differencing values of the latest observations $Z_p(t)$ and of the m historical observations $Z_m(t)$ at v steps ahead as the TC model does.

Step 3. Define the similarity by a spatial threshold

Same as the first part screening by the spatial threshold in STC model. For example, $Z_1(t)$, $Z_2(t)$, $Z_3(t)$ and $Z_4(t)$ are selected (Figure 5-5) because they are within the spatial threshold. $Z_M(t)$ is excluded because $Z_p(t) - Z_m(t)$ is larger than the spatial threshold value. Let M_3' be the number of the historical observations being selected by the screening through threshold ε_s

Step 4. Perform the reasoning

IF $\left|\zeta_{pn}[t-(n-1)\tau] - \zeta_{mn}[t-(n-1)\tau]\right| \le \varepsilon_t$

THEN $\left|\Delta\theta_{pn}(s) - \Delta\theta_{mn}(s)\right|$ is "fuzzy proportion" to $\left|\Delta\theta_{pn}(t) - \Delta\theta_{mn}(t)\right|$

(5-13)

Step 5. Calculate the similarity membership degrees

Based on the fuzzy proportional reasoning, as shown in Figure 5-6, each membership degree (ω_{mn}) can be estimated as follows:

$$\omega_{mn} = \frac{\left|\Delta\theta_{pn}(t) - \Delta\theta_{mn}(t)\right|}{\delta_n(t)} \tag{5-14}$$

where $\delta_n(t) = \max\{z_m(t) - z_m(t-v)\}$, m=1,2,..., M_3'

Step 6. Estimate the "increments" for prediction

Calculate the future differencing values for the latest observations. Use eq. (5-15) to calculate the estimator $\Delta\hat{\theta}_{SC}(s)$ from the differencing value $\Delta\theta_{mn}(s)$ obtained from eq. (5-13).

$$\Delta\hat{\theta}_{SC}(s)=\frac{\sum_{m=1}^{M_3'}\omega_{mn}\Delta\theta_{mn}(s)}{\sum_{m=1}^{M_3'}\omega_{mn}} \tag{5-15}$$

Step 7. Calculate the predicted value for the latest observations

$$\hat{\zeta}_{pn}(t+s)=\zeta_{pn}(t)+\Delta\hat{\theta}_{SC}(s) \tag{5-16}$$

5.2 Empirical Results

5.2.1 Data

Our empirical one-minute traffic flow data are directly drawn from 16 detector stations of the United States I-35 Freeway in Minneapolis, Minnesota. Averages of the lane-specific traffic counts are accumulated over one-minute period. At each station the minute-flow data for ten workdays' morning peak hours from 6 am to 9 am are extracted. Since 20 samples are missing on the last day at some stations, for consistency, we only take 1,780 samples for each station, of which 1,640 samples are used for model construction and the remaining 140 samples are for prediction performance evaluation. The average flow rates for these 16 stations range from 16.8 to 33.8 vehicles per minute per lane, or equivalently, with average headways from 3.57 seconds (a moderate flow) to 1.78 seconds (a saturated, near capacity, flow).

Three parameters of the TC model, including delay time (τ), embedding dimension (N) and temporal threshold (ε_t), need to be determined in advance. While for the STC and SC models, additional parameter, spatial threshold (ε_s), must be determined. The delay time is determined by the autocorrelation function (*ACF*) as illustrated in Fig. 8 The appropriate delay time is the value when *ACF* reaches zero at the first time. At station 32, for instance, the appropriate delay time is 44 minutes. To determine appropriate thresholds and embedding dimension, 27 combinations (ε_s =4, 5, 6; ε_t =4, 5, 6; *N*= 5, 6, 7) are attempted for each station. The spatial threshold, temporal threshold and embedding dimension that minimize the prediction errors for each model are used for further comparison. In the present paper, the number of prediction step (*s*) is set equal to 1.

5.2.2 Prediction performance

We use two criteria, root-mean-square percent error *RMSPE* and Theil inequality coefficient *U*, to measure the prediction error. These criteria are defined as follows (Pindyck and Rubinfeld, 1997):

$$RMSPE = \sqrt{\frac{1}{T}\sum_t \left(\frac{\hat{x}_t - x_t}{x_t}\right)^2} \tag{5-17}$$

$$U = \sqrt{\frac{1}{T}\sum_t (\hat{x}_t - x_t)^2} \Bigg/ \left(\sqrt{\frac{1}{T}\sum_t x_t^{\,2}} + \sqrt{\frac{1}{T}\sum_t \hat{x}_t^{\,2}}\right) \tag{5-18}$$

where $\hat{x}_t$, x_t respectively represent the predicted and observed values at time *t* and T is the number of observations. *RMSPE* is a good indicator for the comparison of prediction errors by different models. The smaller the *RMSPE* is, the higher accuracy the model will predict. The other good indicator *U* can take values between zero and one. The closer to zero *U* is, the more accurate the prediction is. If *U*=0, $\hat{x}_t = x_t$ for all *t* and it is a perfect prediction. If *U*=1, on the other hand, the predictive performance is as bad as it possibly could be. Note that the numerator (without square root) of *U* can be further decomposed into the following three proportions: the bias (U^M), the variance (U^S), and the covariance (U^C) (Pindyck and Rubinfeld, 1997):

$$U^M = (\bar{\hat{x}} - \bar{x})^2 \Big/ (1/T)\sum_t (\hat{x}_t - x_t)^2 \tag{5-19}$$

$$U^S = (\hat{\sigma}_t - \sigma_t)^2 \Big/ (1/T)\sum_t (\hat{x}_t - x_t)^2 \tag{5-20}$$

$$U^C = 2(1-\rho)\hat{\sigma}_t\sigma_t \Big/ (1/T)\sum_t (\hat{x}_t - x_t)^2 \qquad (5\text{-}21)$$

where $\bar{\hat{x}}^2, \bar{x}^2, \hat{\sigma}_t, \sigma_t$ are the means and standard deviations of the series $\hat{x}_t$ and x_t, respectively, and ρ is their correlation coefficient. The bias proportion U^M is an indication of systematic error; the variance proportion U^S indicates the ability of the model to replicate the degree of variability; the covariance proportion U^C measures unsystematic error. We would hope that both U^M and U^S would be close to zero and U^C close to one. For any value of $U > 0$, the ideal distribution of inequality over the three prediction error sources is $U^M = U^S = 0$ and $U^C = 1$. A large value of U^M or U^S (say, above 0.2) would mean that a systematic bias is present or the fluctuation of actual time series data considerably differs from that of forecasted data; thus the model should be revised (Pindyck and Rubinfeld, 1997).

Table 5-1 reports the prediction results and information of *RMSPE* and *U* (with three prediction error sources) for the three models. Overall speaking, station 32 performs the worst in prediction while station 52 is the best for our three prediction models. The possible reason is that station 32 may contain unusual traffic pattern (e.g., long-duration incident due to road construct or bad weather during the ten-day observations) in its original flow time series. For TC model, the value of *U* ranges from 0.099 to 0.197 and the value of *RMSPE* ranges from 0.106 to 0.281. For STC model, the value of *U* ranges from 0.089 to 0.180 and the value of *RMSPE* ranges from 0.106 to 0.224. For SC model, the value of *U* ranges from 0.079 to 0.171 and the value of *RMSPE* ranges from 0.106 to 0.209. Such small values for *RMSPE* and *U* suggest that our proposed three models have predicted rather satisfactorily. We further investigate the sources of prediction errors by examining both the bias and variance proportions for *U* statistic, which are far less than 0.2 at all stations, robustly indicating that our prediction models can successfully capture the trends and fluctuations of one-minute flow dynamics.

In general, the STC model performs somewhat better than the TC and SC models in low-flow conditions; SC model is slightly superior to the STC model, which performs better than the TC model in medium- to heavy-flow conditions. Figure 5-10 relates the prediction errors to the traffic volumes. We find that both *U* and *RMSPE* decline somehow with the increase of traffic volume, implying that our proposed three prediction models perform better in heavier flow conditions than in lighter ones. Taking the lightest traffic volume at station 32 (the worst prediction case) and the highest traffic volume at station 55 (the second-best prediction case) as examples, Figure 5-8 and 5-9 compare their 140 validation samples between the predicted and observed one-minute flow time series data. Both Figures 5-8 and 5-9 have demonstrated the powerful prediction capability of our proposed models, which are verified by the above-mentioned low *U* statistic with very small bias and variance proportions.

5.3 Sensitivity Analysis

We conduct a sensitivity analysis for the STC model by varying the temporal threshold value ε_t under the best combination of ε_s and *N*. Taking the worst case (station 32) as an example, the result is shown in Figure 5-11, which indicates that as the temporal threshold ε_t is enlarged, the prediction errors for STC model tend to decrease and converge to the SC model. It concludes that if we relieve the temporal restraint, the STC model will perform equally well as the SC model although both models have utilized somewhat different prediction reasoning rationales.

Furthermore, Figure 5-12 presents another sensitivity analysis for the STC model by varying the spatial threshold value ε_s under the best combination of ε_t and *N*. We also note that as the spatial threshold ε_s is enlarged, the prediction errors of STC model tend to increase and converge to the TC model. Theoretically, we can view TC model as a special case of STC model if ε_s approaches to arbitrarily large. The sensitivity analysis agrees to this underline theory.

As explained in the models development, the TC model does not rule out any historical trajectories that are far away from the present observed data in the reconstructed state space. It only rules out the trajectories beyond a temporal threshold value ε_t, which are viewed temporal dissimilarity. One may assert that the distant historical trajectories would be more dissimilar than the nearby trajectories to the present data. If this is true, the predictive power of TC model must be inferior to the STC model. Our empirical cases study has validated this assertion.

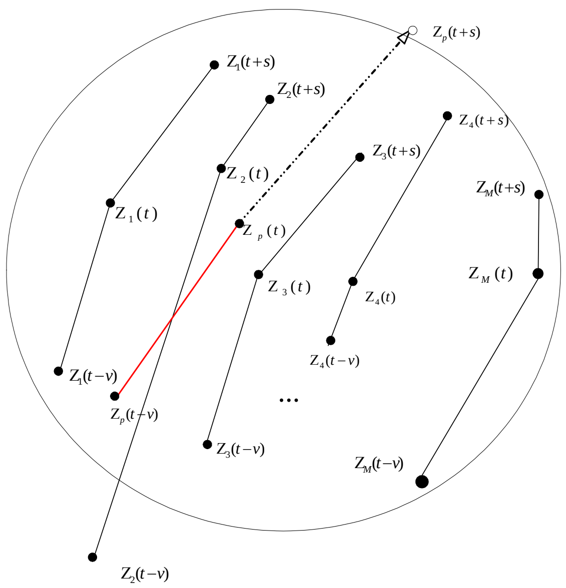

Figure 5-1 Selection of “similar trajectories” by a temporal threshold (Assume M_1' =3; i.e., trajectories 1, 3, and M are selected)

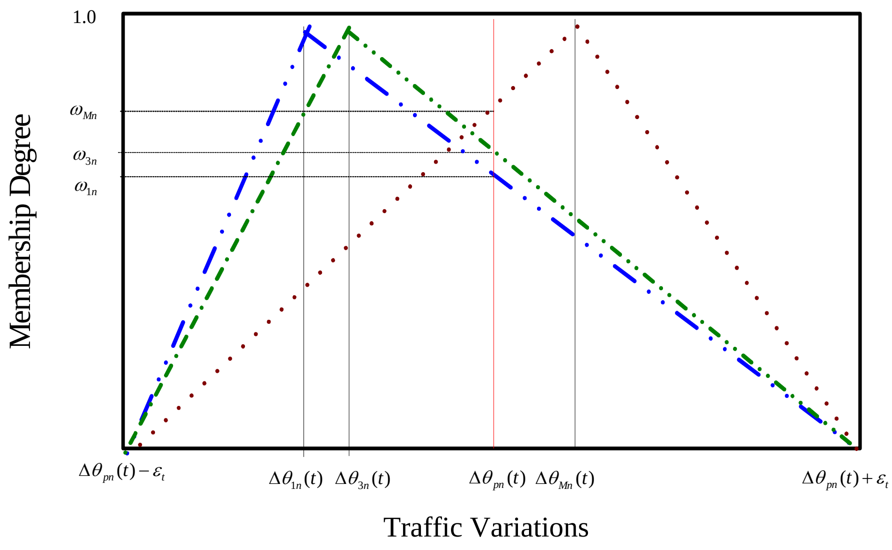

Figure 5-2 Similarity membership degrees for TC Model (M_1' =3 from Fig. 2)

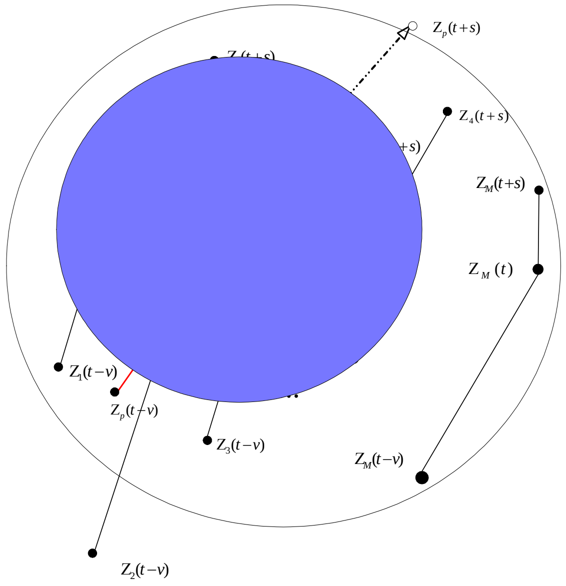

Figure 5-3 Selection of "similar trajectories" by spatial and temporal thresholds (Assume M_2'=2; i.e., trajectories 1 and 3 are selected)

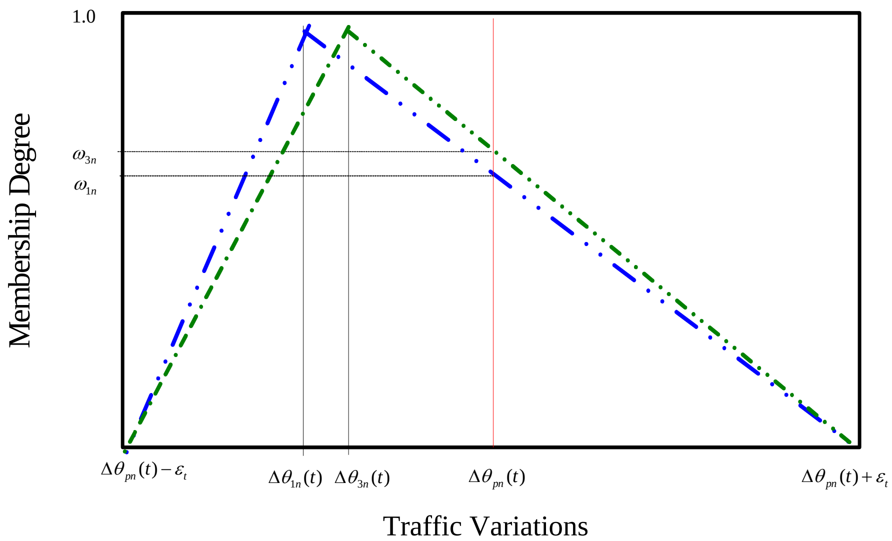

Figure 5-4 Similarity membership degrees for STC model ($M_2' = 2$ from Fig. 4)

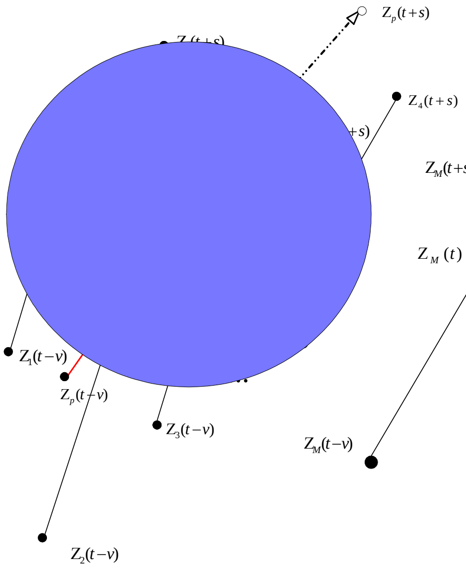

Figure 5-5 Selection of “similar trajectories” by spatial threshold (Assume M_3'=4; i.e., trajectories 1, 2, 3 and 4 are selected)

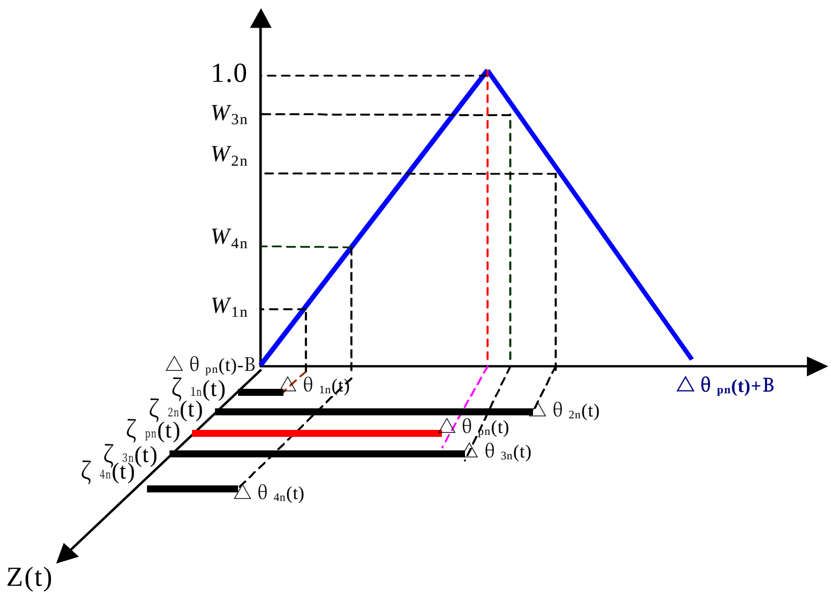

Figure 5-6 Similarity membership degrees for SC model ($M_3' = 4$ from Fig. 6)

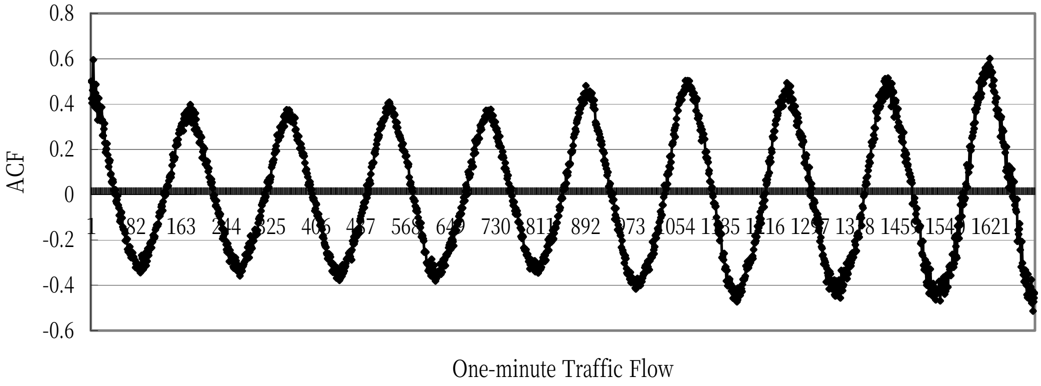

Figure 5-7 Autocorrelation function
(Station 32, for example)

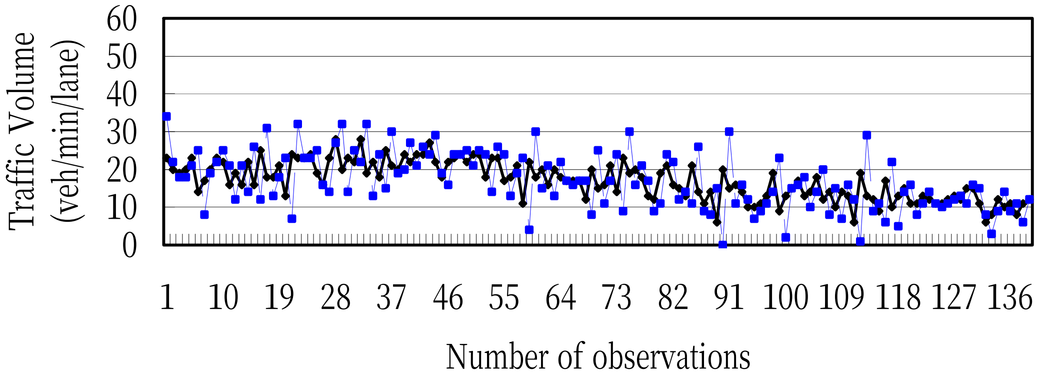

(a) TC Model

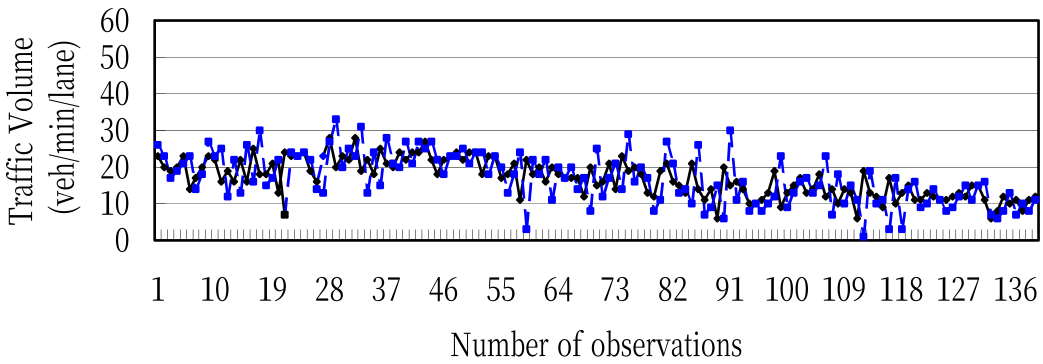

(b) STC Model

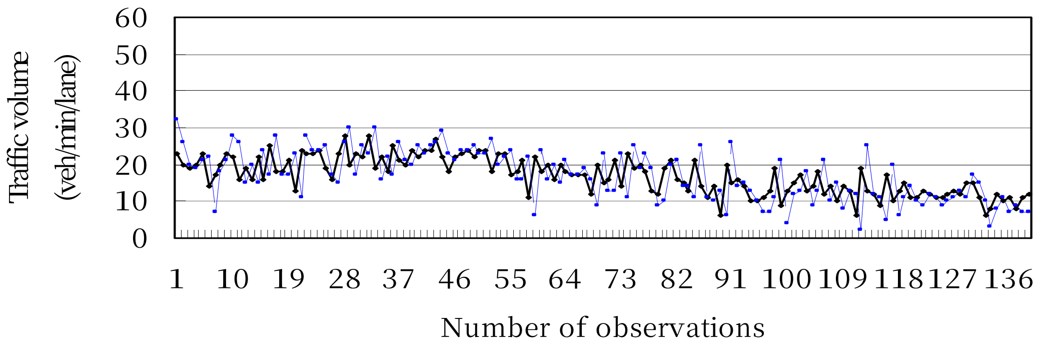

(c) SC Model

(Solid line is the observed data; dot line is the predicted data)

Figure 5-8 Comparison of predicted and observed traffic flows at the lightest traffic volume station 32 (the worst prediction case)

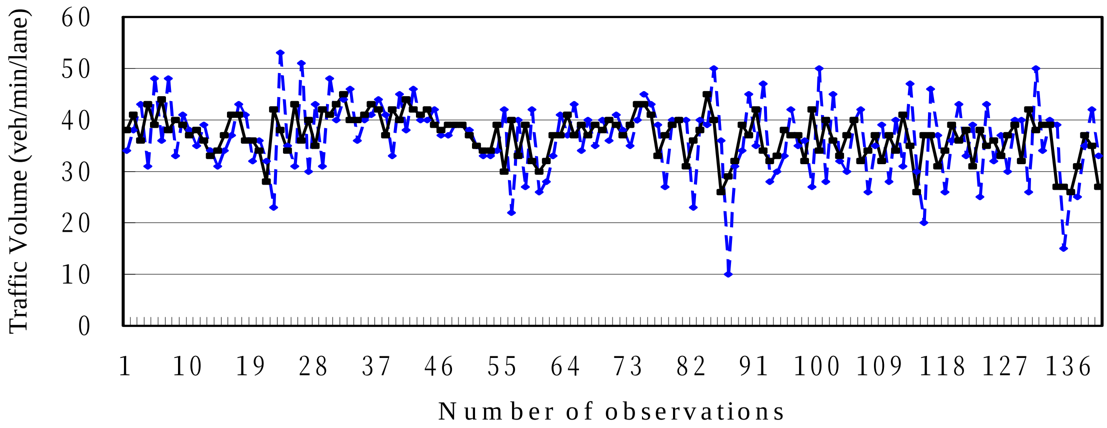

(a) TC Model

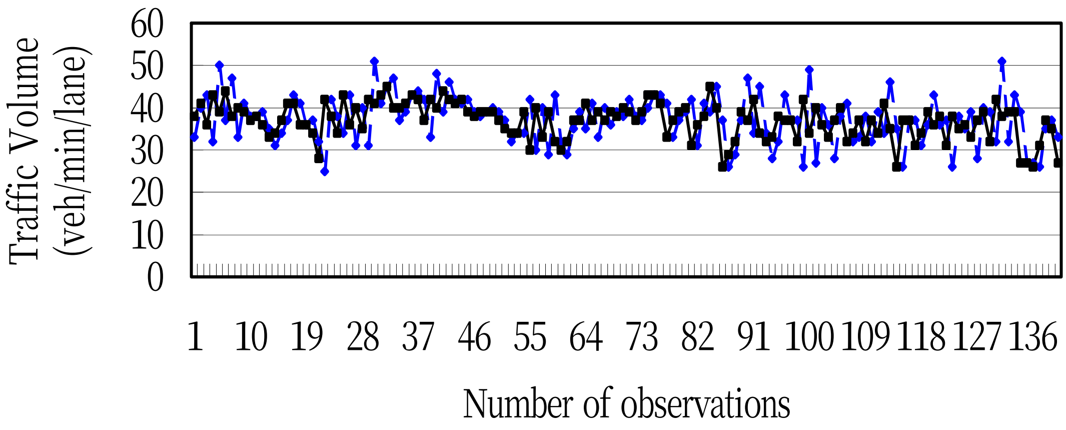

(b) STC Model

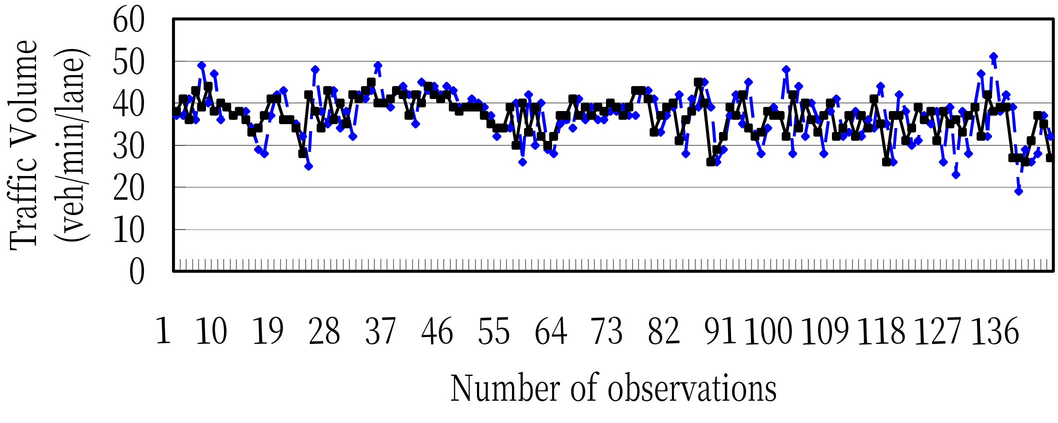

(c) SC Model

(Solid line is the observed data; dot line is the predicted data)

Figure 5-9. Comparison of predicted and observed traffic flows at the highest traffic volume station 55

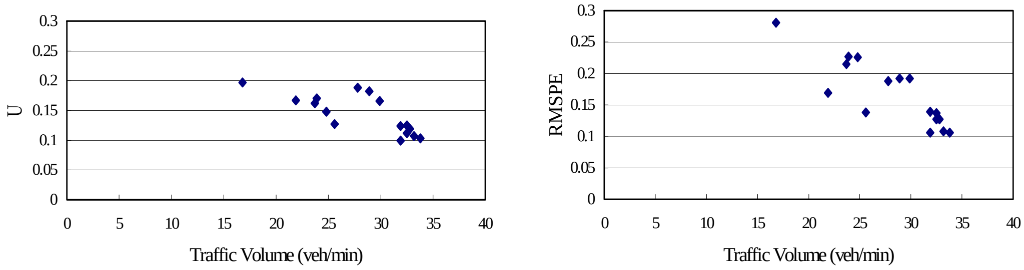

(a) TC Model

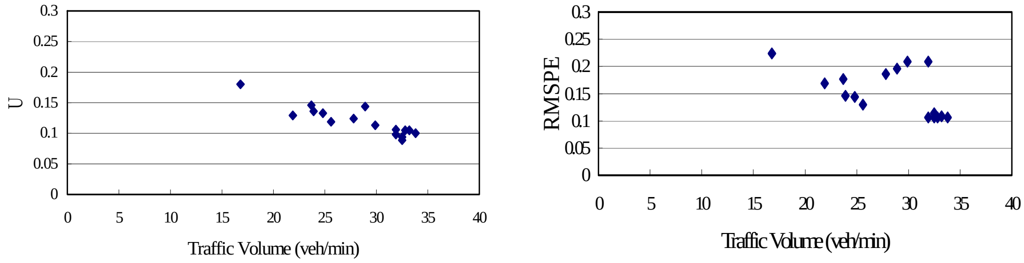

(b) STC Model

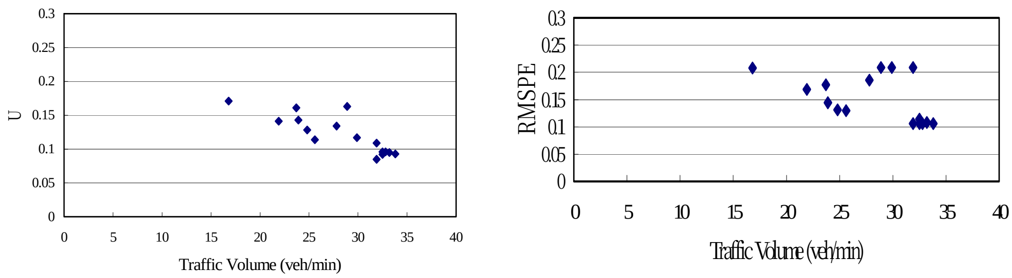

(c) SC Model

Figure 5-10 Prediction errors with respect to traffic volumes

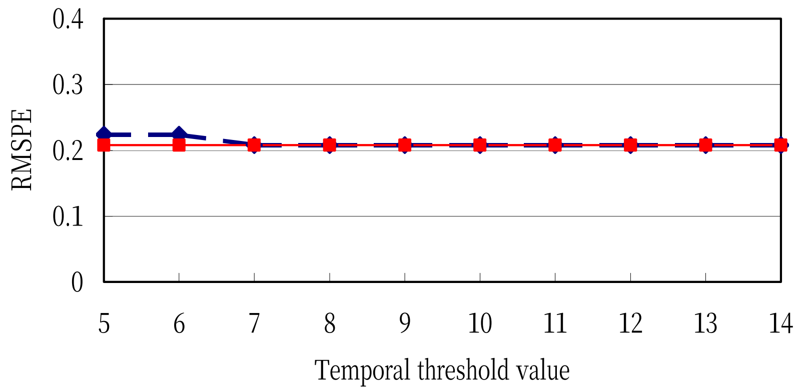

(Solid line is the SC model; dot line is the STC model)
Figure 5-11 Sensitivity analysis for temporal threshold value ε_t
(Station 32, for example)

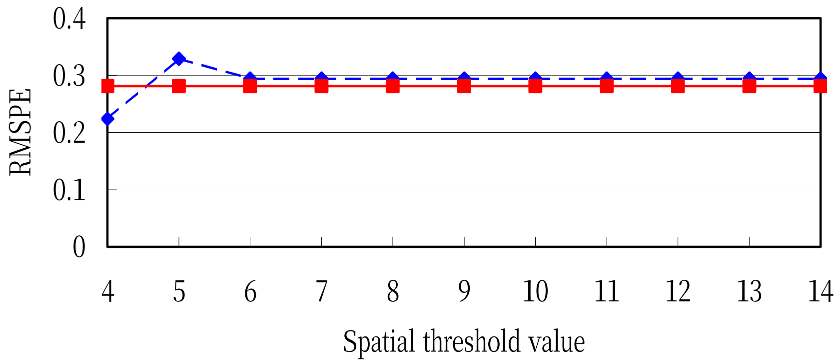

(Solid line is the TC model; dot line is the STC model)
Figure 5-12 Sensitivity analysis for spatial threshold value ε_s
(Station 32, for example)

Table 5-1 Prediction performances for the three models and sources of prediction errors

Station no.	Traffic volume (veh/min/lane)	Model	ε_s	ε_t	Embedding dimension	Delay time τ (minutes)	*RMSPE*	*U*	Sources of prediction error		
									U^M	U^S	U^C
32	16.8	TC	-	6	6	44	0.281	0.197	0.000	0.106	0.894
		STC	4	5	6		0.224	0.180	0.001	0.076	0.923
		SC	5	-	6		0.208	0.171	0.000	0.079	0.921
49	21.9	TC	-	6	7	27	0.169	0.167	0.000	0.151	0.849
		STC	4	4	7		0.169	0.129	0.002	0.021	0.977
		SC	4	-	7		0.169	0.141	0.002	0.056	0.942
45	23.7	TC	-	6	5	22	0.215	0.162	0.001	0.156	0.843
		STC	4	4	7		0.177	0.146	0.000	0.019	0.981
		SC	4	-	7		0.177	0.161	0.009	0.035	0.956
48	23.9	TC	-	6	5	25	0.227	0.170	0.000	0.153	0.847
		STC	4	4	6		0.146	0.136	0.000	0.016	0.984
		SC	4	-	5		0.144	0.143	0.000	0.092	0.908
44	24.8	TC	-	6	5	20	0.226	0.148	0.001	0.142	0.857
		STC	4	6	6		0.144	0.133	0.002	0.030	0.968
		SC	5	-	5		0.131	0.128	0.000	0.075	0.925
50	25.6	TC	-	5	5	23	0.138	0.127	0.001	0.147	0.852
		STC	4	6	7		0.130	0.119	0.001	0.045	0.954
		SC	4	-	7		0.130	0.114	0.002	0.018	0.980
39	27.8	TC	-	6	5	28	0.188	0.188	0.000	0.164	0.836
		STC	4	5	7		0.186	0.124	0.001	0.003	0.996
		SC	4	-	7		0.186	0.134	0.000	0.009	0.991
43	28.9	TC	-	6	5	29	0.192	0.182	0.002	0.167	0.831
		STC	4	4	6		0.196	0.144	0.001	0.005	0.994
		SC	4	-	7		0.209	0.163	0.005	0.050	0.945
41	29.9	TC	-	6	5	29	0.192	0.166	0.001	0.176	0.823
		STC	4	4	7		0.209	0.113	0.002	0.002	0.996
		SC	4	-	7		0.209	0.117	0.001	0.002	0.997
42	31.9	TC	-	6	6	29	0.139	0.124	0.001	0.185	0.814
		STC	4	6	7		0.209	0.106	0.006	0.006	0.988
		SC	5	-	7		0.209	0.109	0.003	0.005	0.992
52	31.9	TC	-	6	5	27	0.106	0.099	0.004	0.111	0.885
		STC	4	5	5		0.106	0.098	0.013	0.107	0.880
		SC	7	-	5		0.106	0.085	0.006	0.023	0.971
51	32.5	TC	-	6	7	24	0.137	0.125	0.001	0.174	0.825
		STC	4	5	6		0.114	0.089	0.000	0.007	0.993
		SC	4	-	6		0.114	0.096	0.002	0.024	0.974
53	32.5	TC	-	6	6	27	0.127	0.112	0.002	0.127	0.871
		STC	4	6	5		0.106	0.094	0.001	0.072	0.927
		SC	5	-	5		0.106	0.092	0.001	0.056	0.943
54	32.8	TC	-	6	6	27	0.127	0.119	0.001	0.123	0.876

		STC	4	6	5		0.106	0.105	0.000	0.081	0.919
		SC	5	-	5		0.106	0.096	0.006	0.028	0.966
56	33.2	TC	-	6	5	28	0.108	0.107	0.003	0.142	0.855
		STC	4	6	5		0.108	0.105	0.008	0.134	0.858
		SC	5	-	5		0.108	0.095	0.005	0.061	0.934
55	33.8	TC	-	6	5	27	0.106	0.103	0.003	0.155	0.842
		STC	4	5	5		0.106	0.100	0.002	0.046	0.952
		SC	5	-	5		0.106	0.093	0.000	0.061	0.939

Note: The bias proportion U^M is an indication of systematic error; the variance proportion U^S indicates the ability of the model to replicate the degree of variability; the covariance proportion U^C measures unsystematic error. For a satisfactory prediction model, both *RMSPE* and *U* values should be small (practically, no greater than 0.2). The ideal distribution for $U > 0$ is that both U^M and U^S should be close to zero (less than 0.2) and U^C close to one.